THE ASTROPHYSICAL JOURNAL, 354:428–437, 1990 May 10

WEAKLY BARRED EARLY-TYPE RINGED GALAXIES. II. THE DOUBLE-RINGED S0$^+$ GALAXY NGC 7187

R. BUTA
Department of Astronomy, University of Texas at Austin; and Department of Physics and Astronomy, University of Alabama
Received 1989 August 4; accepted 1989 November 15

ABSTRACT

This paper presents BVR CCD surface photometry of NGC 7187, a southern S0$^+$ galaxy possessing a bright circular inner ring and a faint elongated outer ring. The rings both have a contrast comparable to those observed in typical (R)SB(r)-type galaxies, yet there is no obvious bar crossing the inner ring as in such galaxies. Instead, there are two nearly orthogonal, small oval zones in the bulge region, one of which may be a nuclear bar. The inner ring is a narrow zone of slightly enhanced blue colors and is therefore a place where star formation has been favored in the disk. An asymmetry in the outer ring region suggests that the galaxy has suffered some interaction, possibly associated with membership in a group whose mean redshift is 2500 km s^{-1}.

The origin of the two rings is uncertain. If they are resonance rings, then NGC 7187 would be a possible example of a galaxy which once had a stronger, more important bar than it has now. This bar could have evolved to a more axisymmetric state through an internal interaction, leaving the rings and an inner lens as signatures of its presence. However, the data do not exclude completely the possibility that both rings are a result of a collision or merger/accretion of one or more smaller galaxies with an S0, in which case NGC 7187 would more properly belong into the pure ring galaxy or Hoag-type ring galaxy classes. The main argument against this possibility is that NGC 7187 does not resemble the more prototypical members of those classes. Other considerations are discussed in some detail.

Subject headings: galaxies: individual (NGC 7187) — galaxies: photometry — galaxies: structure

I. INTRODUCTION

The transition region between spirals and S0's provides some of the most interesting ring morphologies in the sky. Between de Vaucouleurs types S0$^+$ and Sa, inner and outer rings are most closed and well defined, and the incidence of double-ringed systems seems higher than elsewhere along the Hubble sequence. Spirals in the range Sab to Sbc also occasionally show both ring types, but more often the features are pseudo-rings made up of part of the spiral pattern. In the very latest types (Sd-Im) inner and outer rings are practically nonexistent. Formation of these kinds of rings has been found to require the presence of a bar and of gas in *n*-body numerical simulations, but it is quite interesting how some of the highest contrast inner and outer rings are observed in S0 galaxies having only the slightest trace of a bar and, presumably, little gas. Such galaxies are not adequately explained by current theories of ring formation, and the purpose of this series is to focus attention on a few extreme examples. The series is based on multicolor CCD surface photometry and began with a study of NGC 3081 (Buta 1990*a*, hereafter Paper I; any reference to NGC 3081 in text will be to this paper).

In this second paper of the series, I present CCD surface photometry of the southern ringed S0$^+$ galaxy NGC 7187. It is a particularly good example of a system with two bright clear rings and almost no sign of a bar. I would like to show that the properties of this object have much in common with other ringed *barred* galaxies but that important differences do exist. Section II describes the observations, while § III describes the morphology. Section IV gives an analysis of the results, and a discussion is provided in § V. Conclusions are given in § VI.

II. OBSERVATIONS

The observations were made with the 3.9 m Anglo-Australian telescope on 1984 October 24 with the RGO CCD camera and an RCA SID 53612 chip having 320 × 512 pixels, each 0″.49 × 0″.49 in size. Three filters were used: Johnson *B* and *V*, and Cousins *R*. Standard reduction techniques were applied as described in Paper I.

Table 1 lists the details of the images. Zero points were calculated from standard stars for all three filters, but for *B* and *V* the photoelectric aperture measurements given in Table 2 could also be used. These measurements were obtained on 1984 May 2 with an EMI 9659 photometer on the 1.0 m telescope of the Siding Spring Observatory. Table 1 compares the zero points determined from both methods. The agreement is good, but it was found that the part of the night when the CCD observations were made was not completely photometric. This will not be a problem for *B* and *V*, but for *R* the photometry will have a zero point uncertainty of at least 0.05 mag. The final images were normalized to the sky level, so that zero points would correspond to the sky brightness, μ_s, in mag s^{-2}. Table 1 also gives estimates of the seeing on each image.

III. MORPHOLOGY AND GROUP MEMBERSHIP

The structure of NGC 7187 is shown in Figure 1 (Plate 21). This is a *V* band image, and it is displayed in true surface brightness (mag s^{-2}) units allowing for zero point (refer to the step scale). The galaxy is an S0$^+$ with two clear rings: a bright sharp inner ring and a faint, diffuse outer ring. What is particularly noteworthy is the difference in the shapes of the two rings:

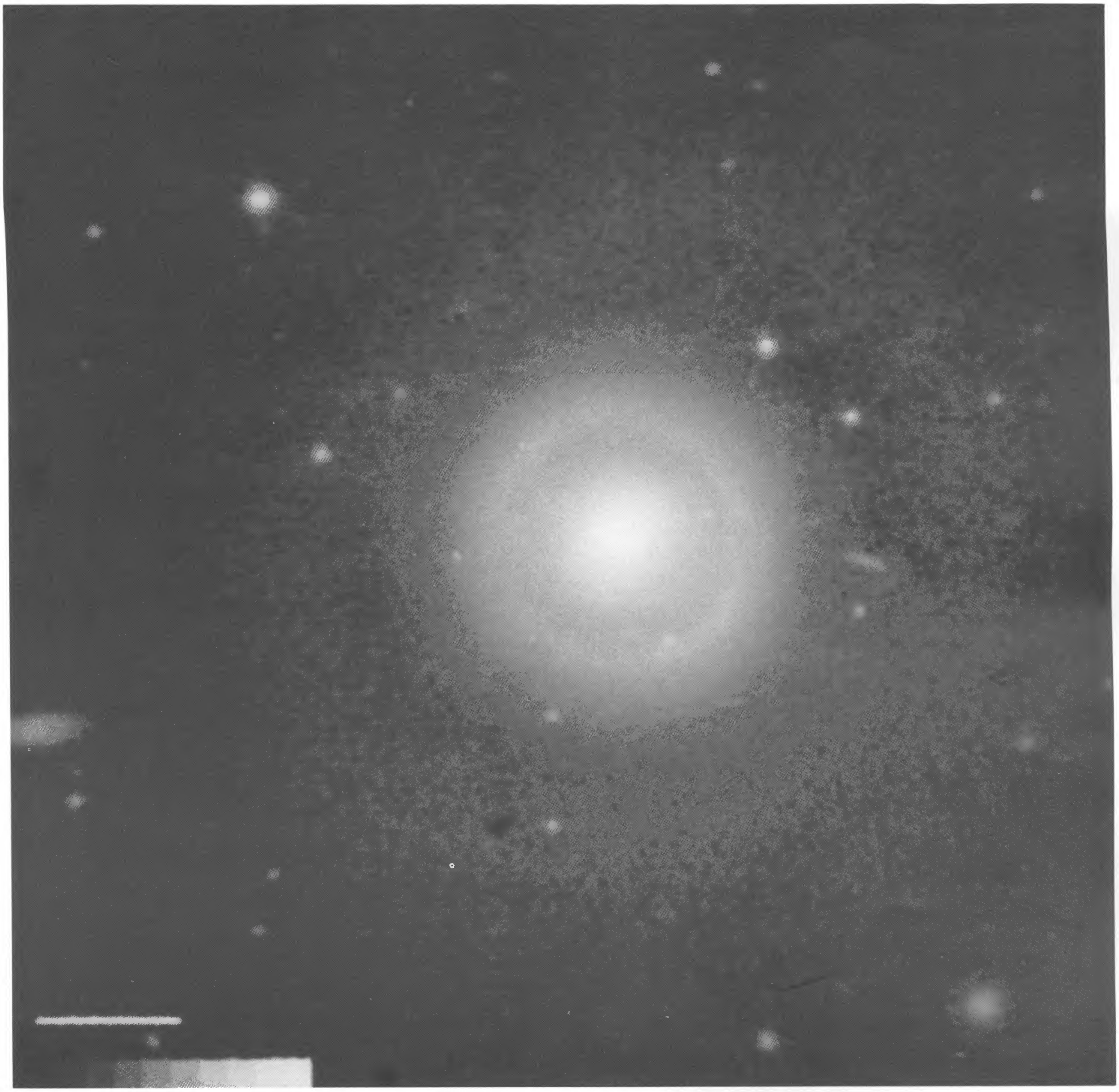

FIG. 1.—V band CCD image of NGC 7187 (225 s exposure). This and Fig. 2 have north at the top and east to the left. The white bar is 20″ in length. The step scale ranges from 17.0 to 27.0 mag s^{-2} in 1.0 mag s^{-2} steps.

BUTA (*see* **354**, 428)

1990ApJ...354..428B

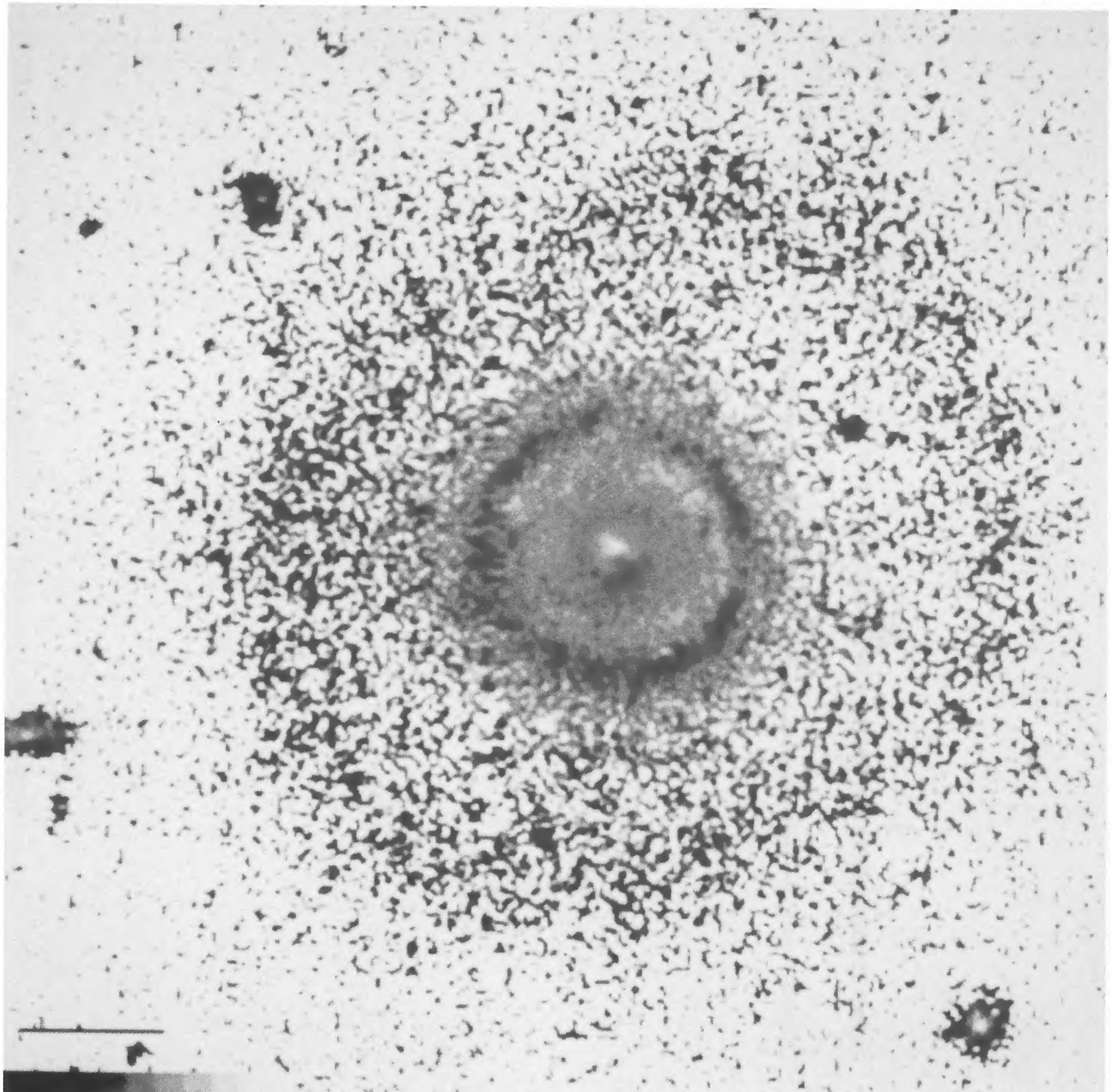

FIG. 2.—$B-R$ color index map of NGC 7187. The dark horizontal bar is 20″ in length. The step scale ranges from $B-R$ = 1.0 (darkest) to 2.0 (lightest) in 0.1 mag steps.

BUTA (*see* **354**, 428)

TABLE 1

OBSERVING LOG OF CCD IMAGES

Filter	Airmass	Sky (ADU)	Exposure (s)	μ_s(Ap.)[a] (mag s^{-2})	μ_s(S.S.)[b] (mag s^{-2})	Seeing (FWHM)
B.....	1.292	128.0	300	22.21	22.19	1".79
V.....	1.309	212.8	225	21.30	21.25	1.62
R.....	1.323	235.5	175	...	20.65	1.61

[a] Based on aperture photometry.
[b] Based on CCD standard stars.

the inner ring looks round compared to the outer ring. No conventional bar appears to cross the inner ring, but the bulge appears slightly oval in shape. The revised Hubble classification is (R)SA(r)0$^+$, but, as will be shown, the galaxy is not completely unbarred.

A $B-R$ color index map is shown in Figure 2 (Plate 22). As for other ringed systems, the inner ring is distinctly enhanced in the blue when compared to its surroundings. There appears to be some variation in color around the ring, but this variation is much smaller than that found in NGC 3081. The outer ring is less enhanced in color by comparison, also as found in NGC 3081. The color characteristics of the rings are quantified in § IV*f*.

Figure 1 indicates that there is some asymmetry in the outer ring region. This ring is not exactly centered on the nucleus, but is miscentered slightly to the northwest. The effect is quantified in § IV*e* and could be due to an interaction. In the Third Reference Catalogue of Bright Galaxies (de Vaucouleurs *et al.* 1989, hereafter RC3), there are nine galaxies within 1° of NGC 7187, seven of which have a similar redshift ($V_\odot = 2670$ km s^{-1} for NGC 7187, and $\langle V_\odot \rangle = 2500$ km s^{-1} for the others). All but one are more than 10 outer ring diameters away, and the closest, ESO 404-21 at 9'.2, has a redshift about 1600 km s^{-1} larger than for NGC 7187. Figures 1 and 2 also show that the galaxy has at least four small companions, though the redshifts of these objects are unknown. It is possible that the outer ring asymmetry of NGC 7187 is due to some interaction associated with its group membership. This is discussed further in § V.

IV. DATA ANALYSIS

a) *Integrated Properties*

As with NGC 3081, the surface photometry was used to measure several integrated parameters (Table 3). The most important, the total magnitude, was obtained by extrapolating an elliptically averaged luminosity profile. The result, $B_T = 13.47 \pm 0.04$, agrees well with $B_T = 13.43$ obtained by Lauberts and Valentijn (1989) based on the ESO sky survey plates. However, my integrated R band magnitude, $R_T = 11.93$, disagrees with theirs by -0.31 mag. This disagreement is much larger than the zero point uncertainty of my R band photometry and could be due to an inadequate calibration of the R band ESO plate used by Lauberts and Valentijn.

The absolute magnitude of NGC 7187 is estimated using its redshift as a distance indicator. The RC3 redshift was measured optically by da Costa *et al.* (1984) and is the only spectroscopic information available for this galaxy. The corrected velocity reduced to the frame of the nearby galaxies (see Buta and de Vaucouleurs 1983) is $V_c = 2502$ km s^{-1} which gives, with $H_0 = 100$ km s^{-1} Mpc^{-1}, an approximate distance of 25 Mpc. If B_T is corrected using RC2 procedures (de Vaucouleurs, de Vaucouleurs, and Corwin 1976), then the absolute magnitude of NGC 7187 is $M_T^0(B) = -18.9$. The galaxy is therefore of relatively low luminosity and is 0.6 mag fainter than NGC 3081.

TABLE 2

APERTURE PHOTOMETRY OF NGC 7187

Aperture	V	$B-V$	$U-B$
23".5.........	13.40	0.94	0.54
47.6.........	12.92	0.96	0.43
94.0.........	12.69	0.89	0.52

TABLE 3

BASIC AND INTEGRATED PARAMETERS[a]

Parameter	Value	Parameter	Value
α(1950)	21^{h}59^{m}48^s	log D_{25}(0'.1)	1.16
δ(1950)	−33°02'42"	log R_{25}	0.12
l	13°.59	θ_{25}	29°
b	−53°.26	$C_{21}(B)$	2.85
SGL	284°.4	$C_{32}(B)$	2.01
SGB	+23°.9	$r_1^*(B)$	0'.081
ESO-B type	S0(r)	$r_e^*(B)$	0'.231
SGC type	(R)SA(r)0$^+$: pec	$r_3^*(B)$	0'.465
Adopted type	(R)SA(r)0$^+$	$\mu_1(B)$	20.57 mag s^{-2}
B_T	13.47	$\mu_e(B)$	22.39 mag s^{-2}
log A_e(0.1).........	0.68	$\mu_3(B)$	24.27 mag s^{-2}
m_e'	12.36 mag m^{-2}	i	26° ± 3°
$(B-V)_T$	0.91	$(B-V)_e$	0.94
$(U-B)_T$	0.46	$(U-B)_e$	0.50
$(V-R)_T$	0.63	$(V-R)_e$	0.61
⟨q(d)⟩	0.90	θ(d)	134°
d(r)	0'.59	d(R)	1'.67
q(r)	0.96	q(R)	0.83
θ(r)	76°:	θ(R)	119°:

[a] Positional information from ESO-B catalog and RC3.

The integrated luminosity and color profiles in circular apertures are shown in Figure 3. These are used to illustrate the quality of the zero point calibrations for V and $B-V$, and were also used to obtain $(B-V)_T$. For $U-B$, a standard RC2 integrated color curve was used to obtain $(U-B)_T$.

Other parameters given in Table 3 are the isophotal dimensions, log D_{25} and log R_{25}, the position angle θ_{25} of this isophote, types from other catalogs (ESO-B: Lauberts 1982; SGC: Corwin, de Vaucouleurs, and de Vaucouleurs 1985) and standard de Vaucouleurs (1948, 1953, 1977) integrated parameters such the equivalent effective radius r_e^*, the surface brightness of the effective isophote μ_e, and the light concentration indices C_{21} and C_{32}. These parameters are calculated from an equivalent luminosity profile in blue light; they indicate a system more concentrated than NGC 3081.

b) *Ring Shapes and Diameters*

Table 3 gives estimates of the apparent shapes and orientations of the inner and outer rings. These refer to the ridge lines of the features as seen in the V band image and were defined visually using a TV display. The inner ring has an axis ratio $q(\mathrm{r}) = 0.96 \pm 0.02$ compared to $q(\mathrm{R}) = 0.83 \pm 0.03$ for the outer ring. The apparent shapes are significantly different, implying that the two rings must have rather different intrinsic shapes or orientations. The inclination can be roughly estimated from the axis ratio of isophotes of the disk beyond the outer ring. The mean axis ratio was found to be $q(\mathrm{d}) = 0.90 \pm 0.02$ from ellipse fits to these isophotes in each passband (§ IV*c*). Assuming an intrinsic flattening of $q_0 = 0.2$ for these isophotes,

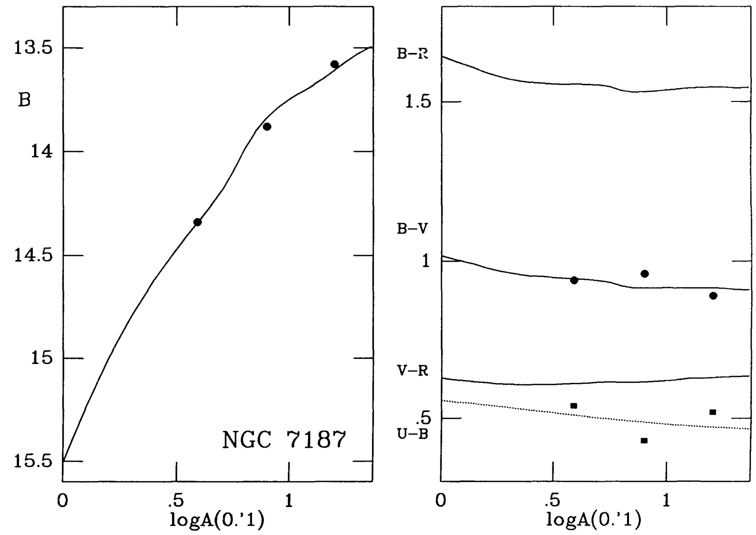

FIG. 3.—Magnitude vs. aperture and color vs. aperture relations for NGC 7187. The solid curves are simulations from the CCD surface photometry, and the data points are measured photoelectric values. The dashed curve for $U-B$ is based on an RC2 standard color curve and was used to extrapolate the integrated color, $(U-B)_T$.

the inclination is $i = 26° \pm 3°$. For a major axis position angle of $\theta(\mathrm{d}) = 134°$, the approximate true ring axis ratios are $q_0(\mathrm{r}) = 0.88$ and $q_0(\mathrm{R}) = 0.90$ in different position angles. The difference in intrinsic position angle is $\sim 53°$.

Using a distance of 25 Mpc, the inner ring has a linear diameter of 4.3 kpc while the outer ring has a diameter of 12.1 kpc. These are small compared to the same types of rings observed in barred galaxies but may be consistent with the lower than average luminosity (Buta and de Vaucouleurs 1982).

c) *Isophotes and Luminosity Profiles*

Isophotes of NGC 7187 based on the V band image smoothed with a $5''.9 \times 5''.9$ box averaging technique are shown in Figure 4. Several features emerge from this map. The first is how the isophote for $\mu_V = 21.5$ mag s^{-2} is more elongated than the inner ring or the bulge isophotes. This is most probably an artifact of a nonuniform surface brightness around the inner ring rather than a weak bar (see § IV*f* and Fig. 11, below). The second feature is how the isophote for $\mu_V = 24.0$ mag s^{-2} is elongated almost perpendicular to the outer ring and is somewhat boxy in shape, a phenomenon also seen in the isophotes of NGC 1433 and NGC 3081. Last, the outer isophotes appear to be getting less elongated with decreasing surface brightness. That is, the shape of the outer ring is not necessarily that of the outer disk.

Higher resolution isophotes of the inner regions are shown in Figure 5. The bulge isophotes have an oval shape whose position angle is a strong function of the radius. The isophotes just beyond the inner ring are actually rounder than most in the bulge, except for the inner 1″ or 2″.

The shapes and orientations are quantified in Figure 6. These are based on ellipse fits, and all three passbands were used with the exception that the B band image could not be used for the center because of an autoguider failure, which led to some slight trailing. From V and R alone we can identify two distinct position angles in the center: one for $1''.3 \leq a \leq 3''.1$ where P.A. = 54°, and one for $5''.1 \leq a \leq 7''.3$ where P.A. = 134°. There are thus two oval zones in the bulge of the galaxy which are nearly orthogonal in projection. It is interesting that the isophotes of the outer disk in the zone $55'' \leq a \leq 62''$ (just outside the ridge line of the outer ring) have a mean position angle $\theta_0 = 134°$, identical with the outer part of the apparent bulge. The shapes of the isophotes (lower panel of Fig. 6) are also very similar in the two regions, with $q \approx 0.90$. If the bulge is a less flattened oblate spheroid than the disk, then this coincidence in shapes is not expected even though the position angle coincidence would be.

The plot of the isophote axis ratios shows a "zig-zag" pattern over the whole disk which is quite unusual. A constant value is never really achieved over any significant range of radius. This makes the inclination and line of nodes very diffi-

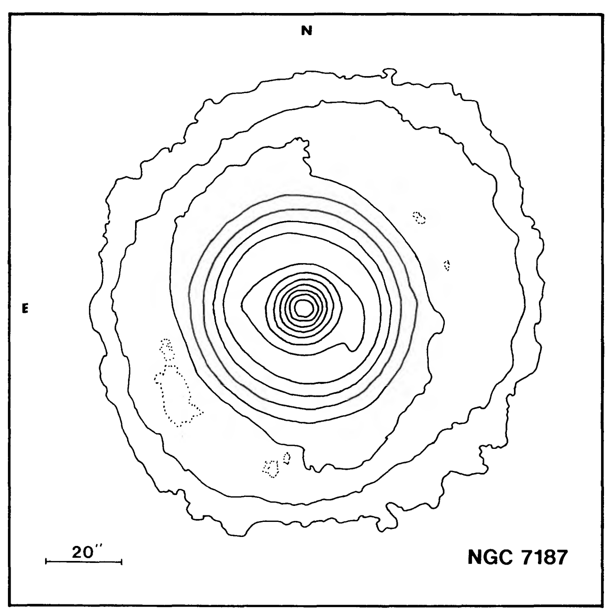

FIG. 4.—V band isophotes of the large-scale structure of NGC 7187. The isophotes were smoothed using a $5''.9 \times 5''.9$ box average. The brightest isophote is at $\mu_V = 18.5$ mag s^{-2}, and each successive isophote is separated by 0.50 mag s^{-2}. The dashed isophotes are in the gap between the inner and outer rings and are at the level $\mu_V = 24.5$ mag s^{-2}.

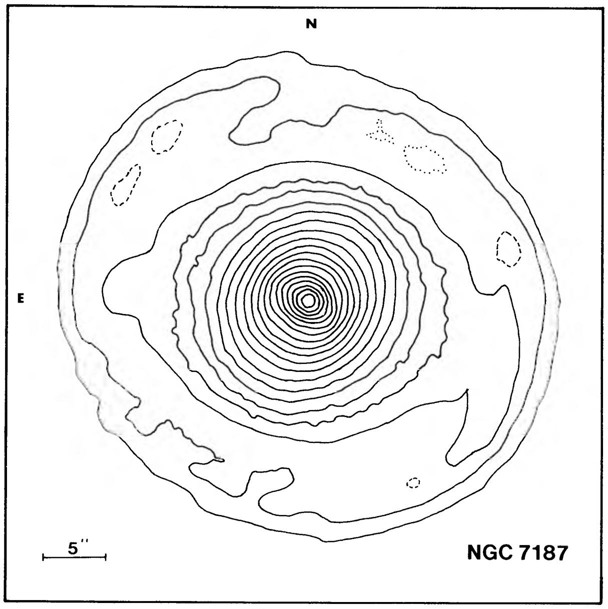

FIG. 5.—*V* band isophotes of the inner regions of NGC 7187, showing the nuclear ovals. The brightest isophote is at $\mu_V = 17.25$ mag s^{-2}, and each successive isophote is separated by 0.25 mag s^{-2}. No smoothing was applied for $\mu_V \leq 21.25$ mag s^{-2}, but for fainter isophotes a 1″.5 × 1″.5 box average was applied. The small dashed contours are at 21.50 mag s^{-2}, while the dotted ones are at 21.75 mag s^{-2}.

cult to determine for this galaxy. The adopted disk parameters in Table 3 are based on means of the outer isophotes in the zones indicated by the dotted lines in Figure 6. It is worth noting that the isophote having $\mu_B = 25.0$ mag s^{-2}, often used for getting inclinations (Bottinelli *et al.* 1983), has an axis ratio of 0.76 and a position angle of 29°, very different from those of the outer disk.

The structure of NGC 7187 was investigated further using a Fourier analysis of the deviations of isophotes from ellipses, as was done for NGC 3081. This is useful for evaluating the barlike nature of the central oval; in NGC 3081 the nuclear bar was found to be a clear pointed oval having significant 4θ amplitude in the residuals about an ellipse fit. The results of a similar analysis for NGC 7187 are shown for the *V* and *R* bands in Figure 7. Only the relative Fourier radius amplitudes, $A_m = (a_m^2 + b_m^2)^{1/2}/a$, for $m = 4$ and 6 are shown. Here a_m and b_m are the sine and cosine amplitudes, respectively, of the deviations of each isophote from its fitted ellipse, whose major axis radius is *a*. There appears to be significant $m = 4$ amplitude between $a = 1''$ and $3''$ associated with the innermost oval. This suggests that this feature is a nuclear bar, just as was seen in NGC 3081. The second inner oval shows much less significant $m = 4$ amplitude, but in the region between this feature and the inner ring, there is significant $m = 4$ and 6 amplitude corresponding to the bar like isophote in Figure 4. In the region just inside the outer ring, more significant $m = 4$ and 6 amplitudes

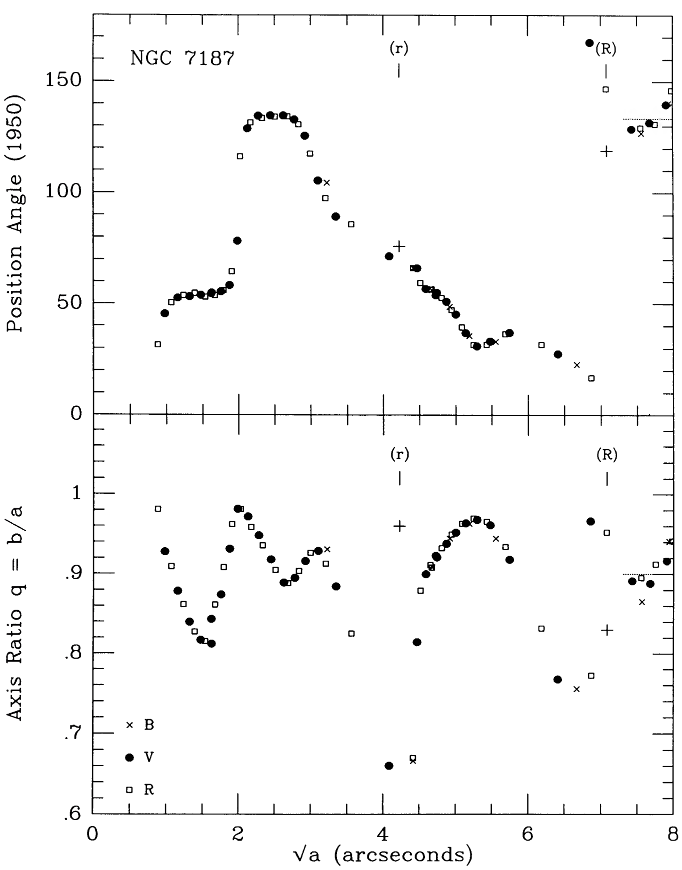

FIG. 6.—Dependence of isophote shapes and orientations on position within NGC 7187, based on ellipse fits. The large plus symbols show values for the ridgelines of the inner ring (r) and outer ring (R).

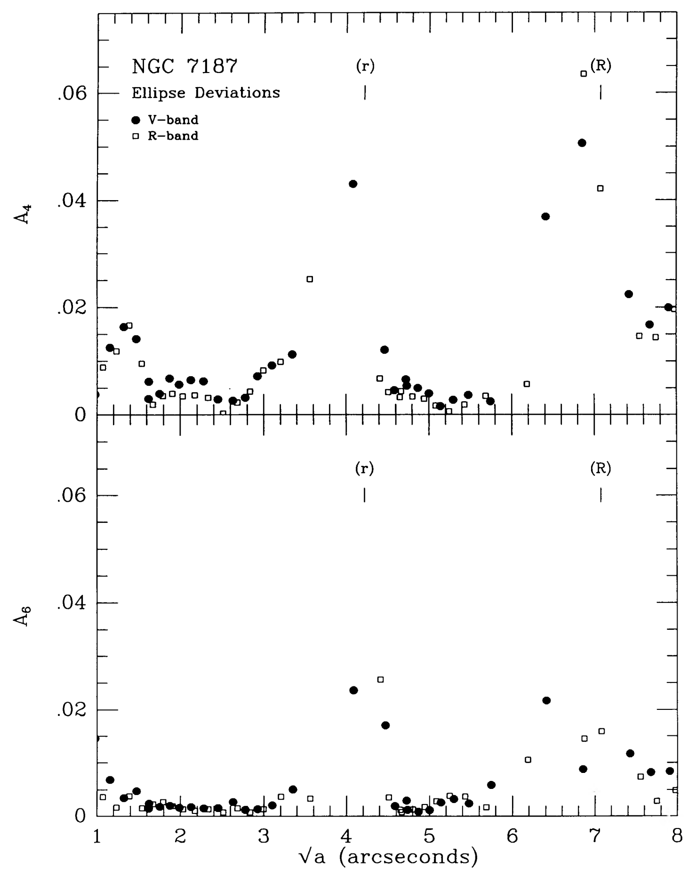

FIG. 7.—Relative amplitudes of the 4θ and 6θ Fourier components for *V* and *R* band isophotes. The major axis positions of the inner ring (r) and outer ring (R) are indicated.

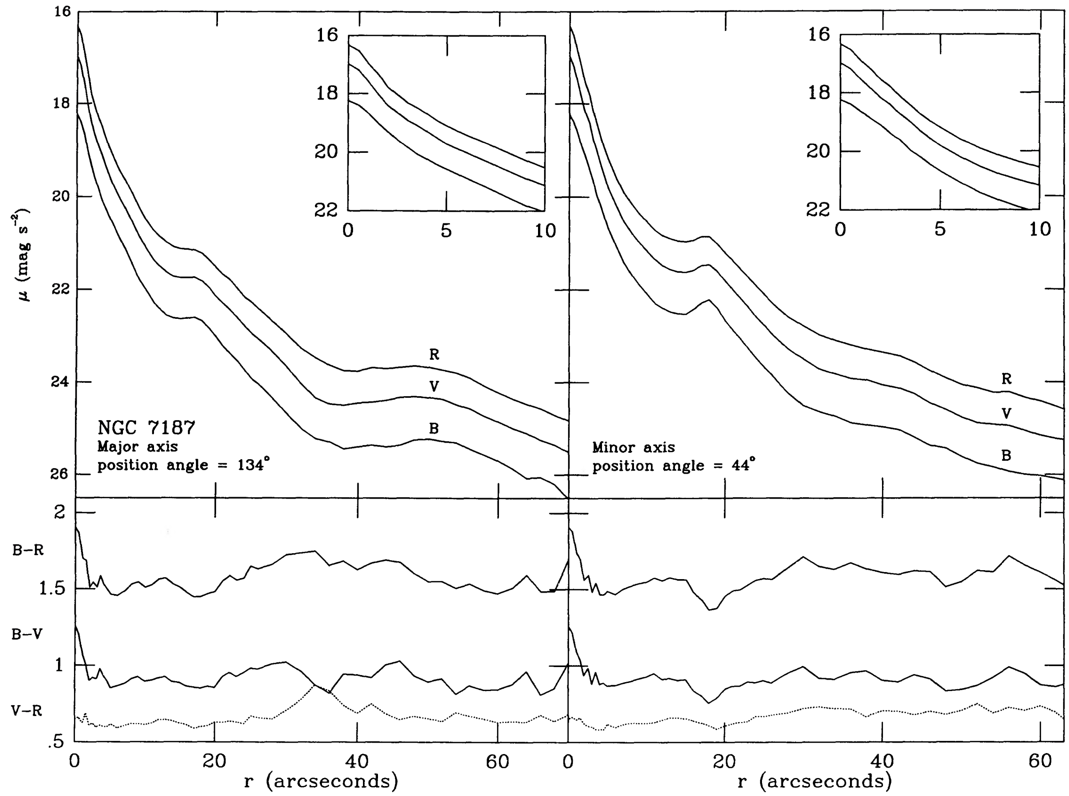

FIG. 8.—Surface brightness and color profiles along the major and minor axes of NGC 7187

are observed associated with the boxy isophote seen in Figure 4.

Luminosity and color index profiles along the major and minor axes are shown in Figure 8. The profiles are typical of a ringed system, but unlike NGC 3081 there is no nuclear ring. As has been observed in similar galaxies, the luminosity distribution beyond the ridge line of the outer ring along the major axis is exponential over the limited range of surface photometry of sufficient precision; elliptically averaged profiles (§ IV*e*) confirm this and show that the exponential character extends to at least $r = 84''$. The extrapolated "central" surface brightness of this region is $B(0)_c \approx 21.35$ mag s^{-2}, very close to the Freeman (1970) mean value. However, since the outer ring of NGC 7187 is so faint, one cannot extend the profiles far enough to be certain that the exponential character continues over a sufficient number of scale lengths.

d) *Profile Decomposition*

The contribution of the bulge to the total light of NGC 7187 is obviously of interest but difficult to derive because of the complex structure inside the inner ring. The V band surface brightnesses along the major and minor axes are plotted versus $r^{1/4}$ in Figure 9. An indiscriminate fit of a de Vaucouleurs law along the major axis was found to predict that most of the light in the gap region between the inner and outer rings is bulge light. I believe this is unrealistic because the image suggests that the disk ought to dominate in this region. In the inner $1''$–$1''.3$ the isophotes become nearly round, and it is probably only in this region where an $r^{1/4}$ bulge, if it exists, truly dominates. To determine its effective radius, the profiles were corrected for seeing using a deconvolution table for the $r^{1/4}$ law compiled by M. Capaccioli (unpublished). In this method, an initial guess is made of the effective radius and the surface brightnesses are corrected in an iterative fashion. Tests were made with different initial guesses to insure that the result did not depend on the guess. The main uncertainty comes from the small radius range that could be used for the fit, the pixel size, and the point spread function (PSF). Several stars were used to estimate the PSF, and the Gaussian width of the inner component of this function was found to be $\sigma_1^* = 0''.69$. The solid lines in Figure 9 show the adopted bulge model derived from the inner 5 pixels along the major axis. The model is applied to both the major and minor axes to show that they agree. The relation is

$$\mu_V^I = 12.271(\pm 0.063) + 5.344(\pm 0.067) r^{1/4} .$$

The constants imply an effective radius of $r_e(V) = 5''.9 \pm 0''.3$ and an effective surface brightness of $\mu_e(V) = 20.60 \pm 0.16$ mag s^{-2}. The errors are internal and do not include the uncertainty in σ_1^* or the complexities due to the profiles themselves. The total luminosity of the bulge can be estimated from

$$L^I = 7.215 \pi I_e r_e^2 ,$$

where I_e is the effective surface brightness in linear units (Simien and de Vaucouleurs 1986). This gives the fractional contribution of the bulge to be $k_I(V) = L_I/L_T = 0.48$. In blue light this k_I would be ~ 0.43 if the color of the spheroid is $B-V = 1.02$. The resulting relative bulge luminosity, $\Delta m_I(B) = -2.5 \log k_I = 0.91$ mag, is near the lower part of the range occupied by S0$^+$ galaxies found by Simien and de Vaucouleurs (1986). This does not mean that the bulge model is correct, only that the result is consistent with galaxies of a similar type.

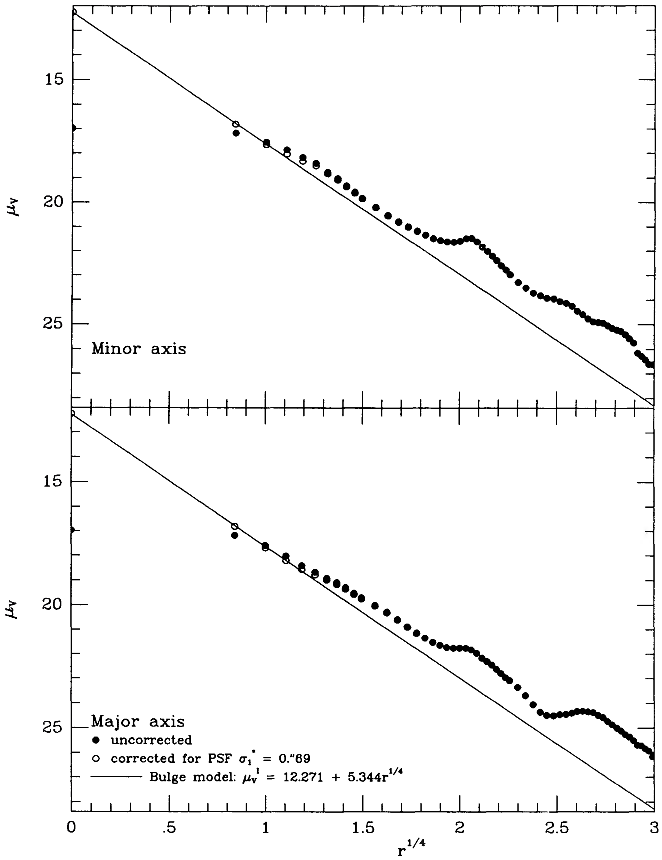

FIG. 9.—Surface brightness profiles vs. $r^{1/4}$ along the major and minor axes of NGC 7187. The filled circles are uncorrected for seeing, while the open circles are corrected for a point spread function whose Gaussian width is $\sigma_1^* = 0.''69$. The solid line shows the adopted bulge model.

e) Elliptically Averaged Profiles and Fourier Intensity Amplitudes

To derive elliptically averaged profiles and relative Fourier intensity amplitudes, I have assumed that the shape and orientation of the disk beyond the outer ring reflect the true inclination and line of nodes of NGC 7187. This assumption leads to the profiles compiled in Table 4. They very much resemble the major axis profiles in Figure 8, and so are not illustrated separately.

Relative R band Fourier amplitudes and phases versus radius normalized to the radius of the isophote having $\mu_B = 25.0$ mag s^{-2} are shown in Figure 10. The $m = 2$ amplitudes are fairly small over most of the disk as expected, and the orthogonal character of the central ovals almost disappears. The amplitudes and phases near the center are, however, not entirely reliable since the true flattening of the bulge has been ignored. More interesting is the $m = 1$ amplitude in the outer disk. For $r/r_{25} < 1$, amplitudes of the odd Fourier terms are virtually negligible, but for larger radii the relative $m = 1$ amplitude reaches 0.3–0.4. This reflects the asymmetry present only in the outer ring region and beyond. The phase of the asymmetry in the region $1.2 \leq r/r_{25} \leq 1.8$ is $\theta_1 = 164° \pm 1°$ with respect to the adopted major axis, which corresponds to a position angle of 300°. This implies that the outer regions are miscentered to the northwest.

f) Ring Colors

The ridge-line colors of the inner and outer rings of NGC 7187 were measured using apertures of 3″ and 10″, respectively. These are illustrated as a function of apparent position angle in Figure 11. Also shown is the azimuthal variation in the surface brightness around the inner ring. Although there appears to be a variation of nearly 0.5 mag s^{-2} in B band surface brightness

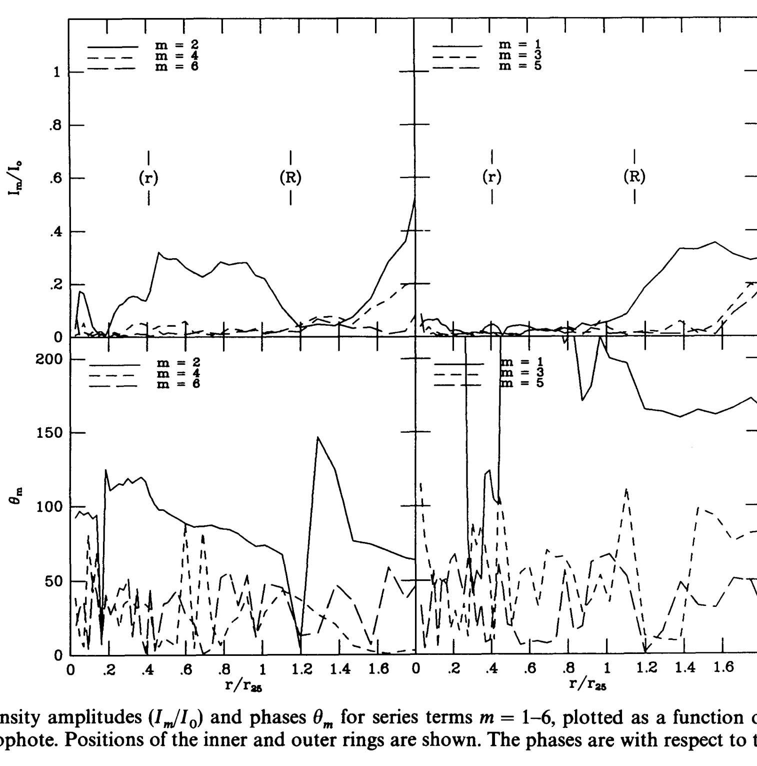

FIG. 10.—Relative Fourier intensity amplitudes (I_m/I_0) and phases θ_m for series terms m = 1–6, plotted as a function of relative radius, r/r_{25}, where r_{25} is the radius of the $\mu_B = 25.0$ mag s^{-2} isophote. Positions of the inner and outer rings are shown. The phases are with respect to the adopted line of nodes position angle, $\theta_0 = 134°$.

TABLE 4

Azimuthally Averaged Profiles[a]

$r('')$	μ_B	$\mu_B - \mu_V$	$\mu_V - \mu_R$
0.0	18.23	1.26	0.65
1.1	18.63	1.08	0.64
2.1	19.19	0.97	0.62
3.0	19.67	0.95	0.60
4.0	20.10	0.91	0.59
5.0	20.50	0.88	0.58
6.0	20.86	0.89	0.59
7.0	21.19	0.90	0.60
8.0	21.49	0.91	0.61
9.0	21.75	0.90	0.62
10.0	21.96	0.90	0.62
11.0	22.15	0.91	0.63
12.0	22.31	0.92	0.64
13.0	22.42	0.92	0.64
14.0	22.49	0.91	0.64
15.0	22.52	0.89	0.64
16.0	22.51	0.87	0.63
17.0	22.50	0.86	0.62
18.0	22.50	0.84	0.61
19.0	22.52	0.82	0.61
20.0	22.61	0.81	0.61
21.0	22.80	0.84	0.61
22.0	23.00	0.88	0.62
24.0	23.36	0.90	0.64
26.0	23.71	0.93	0.65
28.0	24.03	0.93	0.68
30.0	24.33	0.95	0.69
32.0	24.58	0.93	0.71
34.0	24.79	0.91	0.73
36.0	24.93	0.90	0.76
38.0	25.04	0.93	0.74
40.0	25.09	0.94	0.71
42.0	25.09	0.92	0.70
44.0	25.13	0.95	0.68
48.0	25.15	0.92	0.67
52.0	25.28	0.90	0.65
56.0	25.50	0.88	0.68
60.0	25.80	0.94	0.65
64.0	26.07	0.97	0.66
68.0	26.26	0.88	0.70
72.0	26.73	1.09	0.68
76.0	26.93	1.11	0.67
80.0	27.13	0.98	0.69
84.0	27.45	0.97	0.49

[a] In mag s^{-2}.

around the inner ring, that feature shows no clear systematic pattern in the colors.

The mean colors of the inner ring are $\langle B-V \rangle = 0.81 \pm 0.039$ (σ) and $\langle V-R \rangle = 0.60 \pm 0.023$ (σ) based on 23 ridge-line points; those for the outer ring are $\langle B-V \rangle = 0.88 \pm 0.083$ (σ) and $\langle V-R \rangle = 0.66 \pm 0.036$ (σ) based on 62 ridge-line points. The mean $B-V$ colors corrected approximately for galactic extinction, inclination, and redshift using RC2 procedures are 0.71 for the inner ring and 0.78 for the outer ring and are $\sim$0.1 mag redder than for the same rings in NGC 3081. They do not imply exceptionally high star formation rates in the rings (Larson and Tinsley 1978), but it would be useful to obtain an Hα image of NGC 7187 for more reliable estimates of these rates. A few faint patches do appear in the inner ring, particularly in the northeast quadrant, suggesting that H II regions might be present. Note that the corrected integrated colors of the whole galaxy, $(B-V)_T^0 = 0.81$ and $(U-B)_T^0 = 0.40$, are consistent with the average for an S0$^+$ galaxy (de Vaucouleurs 1977).

V. DISCUSSION

The surface photometry shows that NGC 7187 does have some features in common with other ringed, more obviously barred galaxies like NGC 1433 and NGC 3081. There appears to be a small nuclear bar, the surface brightnesses of the rings are similar to those found in barred galaxies, and the inner ring is a sharp zone of bluer colors than its surroundings while the outer ring is a diffuse, broad enhancement. The luminosity profiles are typical of double-ringed galaxies, and in the region between the inner and outer rings, there is a boxy zone that is reminiscent of what is seen in NGC 1433 and NGC 3081. On the other hand, there are the following differences: (1) the absence of an azimuthal color variation around the inner ring; (2) the near circular shape of the inner ring; and (3) the existence of two nearly orthogonal ovals in the bulge region. Assessment of these similarities and differences suggests two possible interpretations: (1) that NGC 7187 is an ordinary double-ringed galaxy whose rings are largely a result of internal dynamics but which has suffered some external perturbation; or (2) that the rings of NGC 7187 may have developed from collisional or merger effects.

a) The Rings as a Result of Internal Dynamics

In this interpretation the rings formed as natural consequences of secular evolution of the gas flow in a barred or ovally distorted galaxy. NGC 7187 must have had sufficiently strong departures from axisymmetry at one time that gas was rearranged into rings which later formed stars. These rings would have occurred near two of the principal orbital resonances expected in a typical galactic disk.

In barred (SB) and moderately barred (SAB) galaxies, photometric properties of rings as well statistics of their apparent relative sizes, shapes, and orientations with respect to bars support their interpretation in terms of bar orbit resonances (Buta 1986*a*, *b*). In double-ringed systems of these types, the ratio of outer to inner ring sizes averages $\sim$2.2 with a standard deviation of 0.5 (Athanassoula *et al.* 1982; Buta 1986*a*) and is close the size ratio expected if outer rings are linked to outer Lindblad resonance (OLR) and inner rings to an ultraharmonic resonance inside corotation (CR), such as the inner 4:1 resonance. Both resonances are known to be important for ring formation from the *n*-body models of Schwarz (1979, 1981, 1984*a*, *b*).

The size ratio of the rings of NGC 7187 is $d(\mathrm{R})/d(\mathrm{r}) = 2.83$, larger than the average for barred galaxies but by less than 2 σ. In the case of a galaxy with a flat rotation curve, the ratio of the radius of OLR to that of the inner 4:1 resonance would be $\sim$2.6. Thus, the observed size ratio of the two rings of NGC 7187 is consistent with the hypothesis that they are related to these two particular orbit resonances if the rotation curve is indeed flat.

It is also noteworthy that the two rings have surface brightnesses very similar to the inner and outer rings of more obviously barred galaxies. For example, the inner ring of NGC 3081 has a ridge-line surface brightness averaging about $\mu_B = 22.4$ mag s^{-2}, and the same average is found for the inner ring of NGC 7187. The outer rings of the two galaxies also have similar surface brightnesses, averaging about $\mu_B = 25.0$–25.5 mag s^{-2}. Similar surface brightnesses were found for the inner and outer pseudo-rings of NGC 1433 (Buta 1986*b*) and for the rings of NGC 7702 (Buta 1990*b*, hereafter Paper IV). In addition, the appearance of the inner ring as a much sharper enhancement than the diffuse outer ring is typical of most double-ringed SB or SAB galaxies.

Finally, the color enhancements observed, particularly for the inner ring, are expected for resonance features. The *n*-body models of Schwarz (1979) showed that a bar or oval distortion can gather gas into rings near resonances, and Combes and

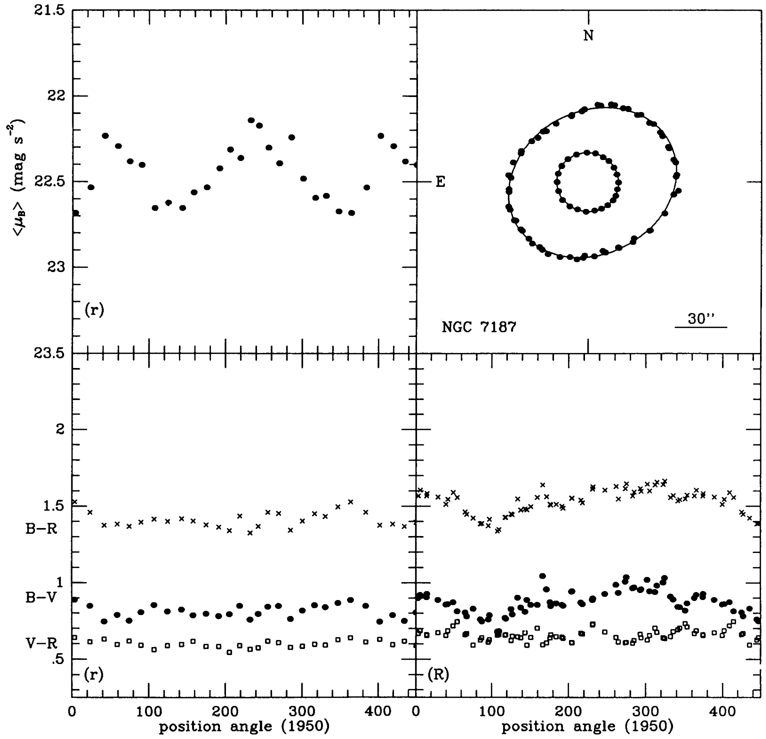

FIG. 11.—Azimuthal ridge-line color and surface brightness profiles of the rings of NGC 7187. The ridge-line positions used are shown in the schematic of the upper right-hand panel. The surface brightnesses are shown only for the inner ring.

Gerin (1985) showed that giant molecular clouds can grow in these regions and lead to enhanced star formation. The star formation rates are not particularly high in the rings of NGC 7187, but are not unexpected given the Hubble stage. The lack of a systematic azimuthal color variation around the inner ring is, however, interesting given its circular shape. The inner ring shows almost no systematic color variation while the more obviously elliptical inner ring of NGC 3081 shows a large color variation. This is what would be expected if the resonance interpretation of the ring is correct (Paper I). However, it is difficult to understand how a near circular resonance ring could have formed when resonances are regions where orbits are supposed to achieve their maximum local eccentricity (e.g., Contopoulos 1979).

The main weakness of the internal dynamics interpretation is the present lack of an obvious bar in NGC 7187. The presence of a central oval nevertheless indicates that there is non-axisymmetry in the bulge of the galaxy. There is definite evidence of highly flattened nuclear ovals in the bulges of SB galaxies (Kormendy 1982*b*), and Zaritsky and Lo (1986) have shown from near-infrared surface photometry that many conventional SA spirals have oval bulges as well. The oval bulges of SB galaxies have been interpreted in terms of orbit properties in the vicinity of the inner Lindblad resonances, an interpretation also favored in Paper I for the bulge of NGC 3081 and in Buta (1986*b*) for the nuclear lens of NGC 1433. It is difficult to make a case for this in NGC 7187 because, unlike the other examples, the nuclear ovals are not really imbedded in a primary bar which crosses the inner ring.

The question then arises as to whether the nuclear bar alone could have been capable of generating rings as conspicuous as those we see in the galaxy. Schwarz (1984*b*) has studied how inner rings form in his *n*-body simulations. He found that his model rings really are resonance features; that is, their location is not directly related to the radius where the bar cuts off, only its pattern speed. If the bar ends far inside CR, a ring does not form in the models at the 4:1 resonance because the perturbation field will not be strong enough near CR for the necessary orbit crossing to occur. Therefore, it is not clear that the inner ring of NGC 7187 could be related to this resonance unless the galaxy once had a more important bar than it appears to have now. The possible causes of bar dissolution are still uncertain, but an interaction with the spheroid seems likely (Kormendy 1979). If originally there was such a bar in NGC 7187, then the small central bar would be an analog of the nuclear bars seen in NGC 1433, NGC 3081, and others discussed by Kormendy (1982*b*). However, had the bar been exceptionally strong, it is unlikely that the inner ring would be so nearly circular as it appears to be. If the galaxy is sufficiently inclined, kinematic observations may allow a more definite assessment of the bar dissolution hypothesis (Kormendy 1984).

If the rings resulted solely from internal dynamics, then an external perturbation would probably have to be invoked to explain the outer ring asymmetry. Perhaps the galaxy suffered a mild encounter in the past associated with its group membership. Since the time scale for the restoring force from perturbations would be longer for the outer ring than for the inner ring, we would expect less asymmetry in the inner regions.

b) The Rings as a Result of External Dynamics

In this hypothesis the rings of NGC 7187 would be solely due to some kind of tidal encounter. There are several possibilities. One is that NGC 7187 suffered a recent retrograde encounter where another galaxy passed close but did not merge. Unpublished *n*-body computer models by P. J. Quinn (1982, private communication, as discussed by Buta 1984) have shown that such encounters can produce multiple (but transient) expanding rings in a disk system if a fairly massive perturber is involved. Toomre and Toomre (1972) actually considered retrograde encounters earlier but concluded that they could produce only mild disturbances to a disk depending on the ratio of masses of perturber and disk. More recently, Thomasson *et al.* (1989) and Byrd *et al.* (1989) have shown how retrograde encounters can produce some aspects of the morphology of NGC 4622, an SA(r) galaxy with a near circular inner ring and a leading arm inside the ring. Since the dominant excitation effect in a retrograde encounter is a 1:1 resonance, any structures resulting from the disturbance are asymmetric, i.e., the ring or rings produced are not necessarily centered, and multiple rings need not have a specific size ratio. The time evolution of such encounters has not been followed sufficiently long in these models to deduce whether they could produce a galaxy like NGC 7187.

A second hypothesis is that NGC 7187 has suffered a collision or merger with another smaller galaxy. The double-oval structure in the central 10″ could be interpreted as isophote twisting due to such a recent merger since there would be an additional subsystem in the bulge. Tidal interactions are known to produce twisting in faint companions (Prugniel, Davoust, and Nieto 1989; Kormendy 1982*a*, p. 115), and early-type galaxies with counter-rotating cores sometimes show twists between two inner subsystems (Kormendy and Djorkovskii 1989). The near circular shape of the inner ring of NGC 7187 could be implying that a direct hit occurred along the line perpendicular to the disk and almost exactly through the center, because off-center or off-axis hits ought to produce more aymmetry (Theys and Spiegel 1977; Struck-Marcell and Appleton 1987*a*). The Fourier analysis discussed in § IV*e* revealed negligible asymmetry in the light distribution of the galaxy to radii more than twice that of the inner ring. This means that the companion would have to be appearing directly projected in the center of the inner ring. Kinematic observations could then shed light on the interpretation, because the relative velocity between the perturber and disk would have to be of the order of 100 km s^{-1} to allow the interpretation to be plausible (e.g., Schweizer *et al.* 1987).

An important question is whether such a direct collision could produce two rings as we observe in NGC 7187. Struck-Marcell and Appleton (1987*a*, *b*) have used cloud-fluid models to simulate a direct hit and predict that two rings, in the form of expanding phase waves, could develop. They believe that the second, smaller ring would be sharper and more enhanced than the first ring because the expanding material in the second ring will encounter gas flowing inward at fairly high velocities from behind the first ring. In addition, they expect that stars born in the rings will fall back toward the center as they age, leading to redder colors behind the shock. High star formation rates are predicted to occur in the rings themselves, especially the second one where bursts are expected. In this picture the outer ring of NGC 7187 would correspond to the first ring of their models and the inner ring to the second. It is interesting that the color index map in Figure 2 reveals a zone of slightly redder colors just inside the inner ring, consistent with the models. However, the reddening could also be due to dust.

Difficulties with the collisional picture are the extremely low probability for a perfectly directly hit, the fact that NGC 7187 currently has lower star formation rates in the rings than might be expected (Struck-Marcell and Appleton 1987*b*), and also the fact that the two rings have different shapes. Although the models can account in a rough way for the difference in the widths of the two rings, the sharpness of the inner ring and diffuseness of the outer ring are characteristics generally found even in barred galaxy rings (e.g., NGC 1433 and NGC 3081). Hence, such characteristics do not necessarily argue for the collisional interpretation of the rings. In addition, NGC 7187 does not resemble the more conventional ring galaxies such as the Cartwheel (Fosbury and Hawarden 1977) or the Vela ring (Taylor and Atherton 1984). In the former object, Struck-Marcell and Appleton (1987*a*) suggest that the larger of two rings is the second wave ring, not the first.

A final possibility is that the rings of NGC 7187 have resulted from accretion of small satellites. Schweizer *et al.* (1987) argued that this is the most plausible interpretation of the beautiful near-circular ring observed in Hoag's Object. Such accretion rings are not usually observed to have a high star formation rate or surface brightness. They can occur not only in polar orbits, as for conventional polar rings (Schweizer, Whitmore, and Rubin 1983), but also in less inclined and even equatorial orbits. In this picture, NGC 7187 may have accreted two dwarf satellites in somewhat differently inclined orbits, in order to account for the different apparent ring shapes. However, the smoothness and general symmetry of both rings, the extreme sharpness of the inner ring, and the low probability of two encounters, may argue against the accretion interpretation in this case. Neither ring morphologically resembles that in Hoag's Object, except for the circular shape of the inner ring. Kinematic data are certainly needed to further evaluate this hypothesis, especially to determine whether the two rings are in the same plane or not.

VI. CONCLUSIONS

The main results of this paper are as follows.

1. NGC 7187 is an S0 galaxy with two clear rings having significantly different apparent shapes. The inner ring is almost perfectly circular and is centered on the nucleus, while the outer ring is symmetric but is miscentered to the northwest. Fourier analysis of the light distribution reveals excellent symmetry to a radius of ~ 2.5 times the inner ring radius.

2. The galaxy has below average luminosity and the rings are small compared to those observed in more typical (R)SB(r)-type galaxies, even though the ratio of their sizes is similar to those in such galaxies. As is typical of double-ringed galaxies, the outer ring is broader and more diffuse than the inner ring.

3. Bulge isophotes reveal the existence of two nearly orthogonal ovals, one having the same shape and position angle as isophotes of the outer disk. The central oval shows significant $m = 4$ deviations from elliptical isophote shapes and could be a nuclear bar. This bar is probably too small and weak to have generated the bright rings seen much farther out.

4. The rings are slightly blue enhancements compared to their surroundings. The inner ring has weak knots and may have H II regions. The mean colors of both rings do not imply exceptionally high star formation rates at the present time.

5. NGC 7187 appears to be a member of a group with a mean redshift near 2500 km s^{-1}. The asymmetry of the outer regions could have arisen from an interaction associated with this membership.

Although these results are ambiguous with regard to the origin of the rings, they do bring attention to the possibility that NGC 7187 is an example of an early-type ringed galaxy whose rings may not have formed from internal dynamics alone, as is believed in the case of more obviously barred galaxies. Surface photometry alone cannot firmly establish the origin of the rings, but from a morphological standpoint the galaxy fits better into the resonance ring picture. However, if the rings are really collisional or merger phenomena, such as those which are believed to characterize ring galaxies, polar ring galaxies, or Hoag-type galaxies, then NGC 7187 is clearly an important example for further study since it does not resemble the prototypes of those classes of rings. Kinematic observations could clarify the issue and are urgently needed.

I would like to thank Deborah Crocker for helpful comments on the manuscript, and especially an anonymous referee for helpful criticisms which allowed me to significantly improve the presentation of this paper.

REFERENCES

Athanassoula, E., Bosma, A., Creze, M., and Schwarz, M. P. 1982, *Astr. Ap.*, **107**, 101.
Bottinelli, L., Gouguenheim, L., Paturel, G., and de Vaucouleurs, G. 1983, *Astr. Ap.*, **118**, 4.
Buta, R. 1984, Ph.D. thesis, University of Texas at Austin.
———. 1986*a*, *Ap. J. Suppl.*, **61**, 609.
———. 1986*b*, *Ap. J. Suppl.*, **61**, 631.
———. 1990*a*, *Ap. J.*, **351**, 62 (Paper I).
———. 1990*b*, in preparation.
Buta, R., and de Vaucouleurs, G. 1982, *Ap. J. Suppl.*, **48**, 219.
———. 1983, *Ap. J.*, **266**, 1.
Byrd, G. G., Thomasson, M., Donner, K. J., Sundelius, B., Huang, T.-Y., and Valtonen, M. J. 1989, *Celestial Mechanics*, **45**, 31.
Combes, F., and Gerin, M. 1985, *Astr. Ap.*, **150**, 327.
Contopoulos, G. 1979, in *Photometry, Kinematics, and Dynamics of Galaxies*, ed. D. S. Evans (Austin: University of Texas Press), p. 425.
Corwin, H. G., de Vaucouleurs, A., and de Vaucouleurs, G. 1985, *Southern Galaxy Catalogue* (Austin: University of Texas Monograph No. 4).
da Costa, L. N., Pellegrini, P. S., Nunes, M. A., Willmer, C., and Latham, D. W. 1984, *A.J.*, **89**, 1310.
de Vaucouleurs, G. 1948, *Ann. d'Ap.*, **11**, 47.
———. 1953, *M.N.R.A.S.*, **113**, 134.
———. 1977, in *The Evolution of Galaxies and Stellar Populations*, ed. B. Tinsley and R. Larson (New Haven: Yale University Observatory), p. 43.
de Vaucouleurs, G., de Vaucouleurs, A., Corwin, H. 1976, *Second Reference Catalogue of Bright Galaxies* (Austin: University of Texas Press) (RC2).
de Vaucouleurs, G., de Vaucouleurs, A., Corwin, H., Buta, R., Paturel, G., and Fouque, P. 1989, *Third Reference Catalogue of Bright Galaxies* (New York: Springer-Verlag, in preparation) (RC3).
Fosbury, R. A. E., and Hawarden, T. G. 1977, *M.N.R.A.S.*, **178**, 473.
Freeman, K. C. 1970, *Ap. J.*, **160**, 811.
Kormendy, J. 1979, *Ap. J.*, **227**, 714.
———. 1982*a*, *Morphology and Dynamics of Galaxies* (Geneva: Geneva Observatory).
———. 1982*b*, *Ap. J.*, **257**, 75.
———. 1984, *Ap. J.*, **286**, 116.
Kormendy, J., and Djorkovskii, S. 1989, *Ann. Rev. Astr. Ap.*, **27**, 235.
Larson, R. B., and Tinsley, B. M. 1978, *Ap. J.*, **219**, 46.
Lauberts, A. 1982, *The ESO-Uppsala Survey of the ESO (B) Atlas* (Munich: European Southern Observatory).
Lauberts, A., and Valentijn, E. A. 1989, *The Surface Photometry Catalogue of the ESO-Uppsala Galaxies* (Munich: European Southern Observatory).
Prugniel, P., Davoust, E., and Nieto, J.-L. 1989, *Astr. Ap.*, **222**, 5.
Schwarz, M. P. 1979, Ph.D. thesis, Australian National University.
———. 1981, *Ap. J.*, **247**, 77.
———. 1984*a*, *M.N.R.A.S.*, **209**, 93.
———. 1984*b*, *Proc. Astr. Soc. Australia*, **5**, 464.
Schweizer, F., Whitmore, B. C., and Rubin, V. C. 1983, *A.J.*, **88**, 909.
Schweizer, F., Ford, W. K., Jedrzejewski, R., and Giovanelli, R. 1987, *Ap. J.*, **320**, 454.
Simien, F., and de Vaucouleurs, G. 1986, *Ap. J.*, **302**, 564.
Struck-Marcell, C., and Appleton, P. N. 1987*a*, *Ap. J.*, **318**, 103.
———. 1987*b*, *Ap. J.*, **323**, 480.
Taylor, K., and Atherton, P. D. 1984, *M.N.R.A.S.*, **208**, 601.
Theys, J. C., and Spiegel, E. A. 1977, *Ap. J.*, **212**, 616.
Thomasson, M., Donner, K. J., Sundelius, B., Byrd, G. G., Huang, T.-Y., and Valtonen, M. J. 1989, *Astr. Ap.*, **211**, 25.
Toomre, A., and Toomre, J. 1972, *Ap. J.*, **178**, 623.
Zaritsky, D., and Lo, K. Y. 1986, *Ap. J.*, **303**, 66.

RONALD J. BUTA: Department of Physics and Astronomy, University of Alabama, Box 870324, Tuscaloosa, AL 35487